

THE MAGNETIC FIELD OF THE NEAREST COOL STAR

A paradigm for stellar activity

CAROLUS J. SCHRIJVER

*Lockheed Palo Alto Research Laboratories (91-30/252)
3251 Hanover Street, Palo Alto, CA 94034-1191, U.S.A.*

Abstract. Looking at the Sun forges the framework within which we try to interpret stellar observations. The stellar counterparts of spots, plages, flux tubes, chromospheres, coronae, etc., are readily invoked when attempting to interpret stellar data. This review discusses a selection of solar phenomena that are crucial to understand stellar atmospheric activity. Topics include the interaction of magnetic fields and flows, the relationships between fluxes from different temperature regimes in stellar atmospheres, the photospheric flux budget and its impact on the measurement of the dynamo strength, and the measurement of stellar differential rotation.

1. Introduction

The interaction of rotation and convection in the stellar interior drives what is referred to as the “dynamo.” This dynamo generates a magnetic field. When part of this field surfaces, it triggers a profusion of processes that are interesting both in their own right and because of the information they may contain about processes in the stellar interior. The Sun is the only star that is near enough to allow detailed observations of its atmosphere. For all other stars one can only see the disk-integrated emission. Distilling information from that stellar signal is facilitated by comparison with the solar outer atmosphere.

Where the Sun offers a detailed view, stars display the variety of basic stellar parameters, such as mass, age, composition, and rotation rate, that allow us to find trends and test theories that address the physics of the invisible layers below the surface. Because of this complementarity, only a combined study of Sun and stars can provide the conceptual framework and the qualitative as well as the quantitative details that are crucial if we are to increase our understanding of stellar magnetic activity. The stellar

aspects are given ample attention in the remainder of this volume. In this introductory paper, I therefore concentrate on solar magnetic activity. I specifically focus on those aspects that are of direct importance to the interpretation of the outer atmospheric emission of “cool” stars, i.e. stars with convective envelopes extending up to their photosphere.

One has to bear in mind that the usefulness of the Sun as a paradigm for stellar magnetic activity is likely to be restricted to a limited range of stellar properties around the solar values. In his summary lecture, Jeff Linsky reminded us that a paradigm can be defined at different levels: one may look for topographical similarities, one may concentrate on processes, or one may focus on the detailed physics. The first class of paradigms is not likely to be useful over a large range of stellar parameters, while the third is too detailed as an initial guide in the relevant domain of radiative magnetohydrodynamics. I therefore focus on the second category and describe the lessons learned from the dynamical solar magnetic field, giving equal weight to the “tools” and “parts” needed for the astrophysical construction kit with which to build a stellar outer atmosphere.

2. The magnetic field in the solar photosphere

The most readily observable component of the solar magnetic field is that which is concentrated in intrinsically strong flux concentrations. That field, with a strength of 1–2 kG, is essentially in equilibrium with the gas pressure of the photospheric plasma surrounding it (e.g. Zwaan, 1987). These flux concentrations, usually referred to as “flux tubes,” are embedded in turbulent convective flows that buffet and displace them. The flux tubes are subjected to continual folding and twisting around themselves and their neighbours, to braking up into smaller fragments, and to merging with other concentrations down to the smallest observable scales, currently at 0.2 arcsec or 150 km (Berger and Title, 1995). These processes result in an apparently random positioning of flux concentrations on length scales below about 2000 km (Schrijver et al., 1992). Fields and flows appear immiscible: upflows occur only where there is no intrinsically strong field (e.g. Spruit et al., 1990) and vice versa. The larger aggregates of magnetic flux (with sizes up to several thousand kilometers) that build the network appear also to be formed by continual random breaking up and merging of smaller concentrations (Schrijver et al., 1996). On yet larger scales, patterns emerge that are formed by the supergranular network and magnetic plages.

The magnetic field reacts back on the flow. This is clearly seen in the so-called abnormal granulation observed in plage regions (Spruit et al., 1990). Whether the field also affects the pattern of the supergranulation is unclear: supergranular openings are not seen inside well-developed, mature

active regions (e.g., Zwaan, 1987), but whether that means that the flow pattern is modified or that only the flux positioning process is different remains to be seen.

Between the strong field an intrinsically weak field is observed. This weak field is thought to be a turbulent field that is generated locally by convective motions (theoretically predicted by, e.g., Durney et al., 1993; observations are reviewed by Keller et al., 1994). The characteristic field strength is ill constrained at present: estimates vary from below 50 G up to 500 G, possibly because there is actually a range of values. Although one cannot rule out that this weak field plays a role in the heating of the chromosphere, its effects are relatively weak and limited to the lower, cooler parts of the outer atmosphere (e.g., Schrijver 1995).

3. Emission from the solar outer atmosphere

With the exception of spot umbrae, every area in the chromosphere that is connected to the intrinsically strong vertical field is brightened (but not all bright areas are necessarily connected to strong field, see below). The magnetically controlled heating must therefore be a quasi-continuous process. The scatter about the relationship between magnetic and radiative flux densities is substantial (e.g., Schrijver et al. 1989). This is caused in part by oscillatory intensity changes, but also, and perhaps more importantly, by the dependence of the chromospheric emission on the detailed field topology and on the dynamics of the magnetic field which moves about in the embedding photospheric plasma (Steiner et al., 1994, present interesting 2-dimensional simulations of footpoint shaking by granulation).

At coronal heights, X-ray emitting arches with cross sections down to the currently achievable resolution of the order of an arcsecond outline the magnetic field. Their very existence as isolated, narrow, bright coronal loops (see for instance the pictures taken with the Normal Incidence X-ray Telescope, Golub et al. 1991) in a field that fills all available space at these heights requires dramatic gradients in the heating on small length scales and therefore a detailed dependence on the boundary conditions given by the dynamic photospheric magnetic field. The movies made from YOHKOH soft X-ray observations show a baffling amount of variability on all time and length scales even when obvious flares are excluded (examples will be accessible at "<http://www.space.lockheed.com/9130.html>", which gives access to the YOHKOH homepage and to the homepages for the SoHO/MDI and TRACE instruments). This variability is predominantly the result of density fluctuations; the temperature and field strength vary much less.

How is the outer atmosphere heated? It appears that two distinct classes of non-radiative heating occur. The "basal heating" is unrelated to the in-

trinsically strong magnetic fields in the photosphere. It appears to be largely the result of dissipation of acoustic waves in the outer atmosphere (reviewed by Schrijver, 1995), although the intrinsically weak field may also play a role. To first order the associated basal emission appears simply to add to the radiation that is associated with the intrinsically strong photospheric fields (see contributions in proceedings of a meeting dedicated to these mechanisms, edited by Ulmschneider et al., 1991). After subtraction of the basal emissions from the observed solar (or stellar) signals, the remaining “excess” emissions are related through power-law relationships for which the power-law index deviates more strongly from unity as the formation temperatures of the compared emissions differ more strongly. Examples of such relationships for solar observations can be found in, e.g., Cappelli et al. (1989) and Schrijver (1992).

One of the many intriguing problems in the field of stellar magnetic activity is the origin of the nonlinearity of the relationships between disk-averaged flux densities in excess of the stellar basal flux. The total emission from the stellar outer atmosphere is, of course, the sum of the emissions from each of the features visible on the disk (and of some beyond the limb). If stellar outer atmospheres would comprise different numbers of otherwise identical features, linear relationships would result. It turns out that in order to understand the nonlinearity, both the small-scale details of the outer atmosphere and the large-scale distribution of magnetic flux in the photosphere are important. The non-linearity for solar data on the scale of individual flux tubes appears to be the combined result of heating, detailed magnetic topology, and radiative transfer (see models by Solanki et al., 1991). The random positioning mentioned in Sect. 2 of flux tubes on scales up to a few thousand kilometers transforms the relationship for individual tubes into essentially the same relationship when observed with the moderate spatial resolution of a few arcseconds (Schrijver, 1993), which is often the achievable limit for solar observations. For the disk-integrated emission, the global field pattern is important. Let me outline what the Sun tells us about this by a description of properties of emergence, dispersal, and disappearance of magnetic flux in the solar photosphere in the subsequent sections. First, let us look at the sources of the field.

4. Properties of bipolar regions

The solar magnetic field surfaces in bipolar active regions with a large range in sizes. The distribution of surface areas A of emerging bipolar regions at maximum development (Fig. 1) resembles a power-law: $N_{\text{em}}(A)dA \propto A^\alpha dA$, with $\alpha = -2.0 \pm 0.1$ (Schrijver and Harvey, 1994). The Sun does not allow a simplification that assumes a “typical” size of active regions or

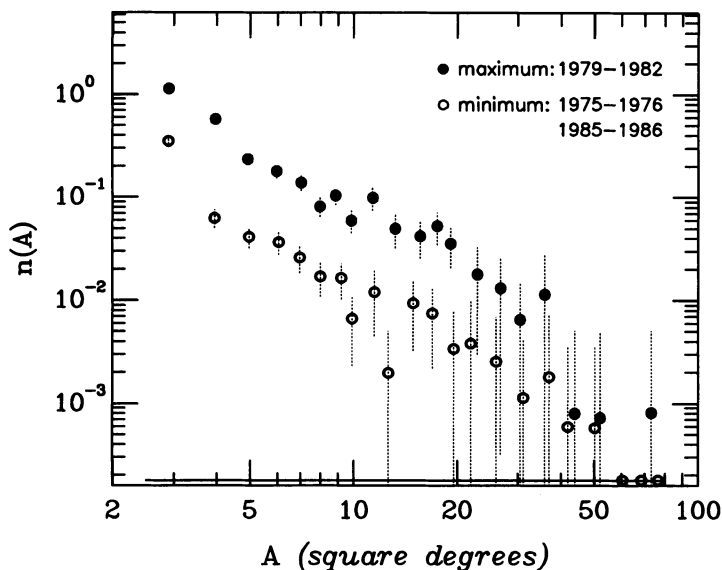


Figure 1. Size distributions of emerging flux regions measured at maximum development (from Harvey and Zwaan, 1993) for cycle maximum and minimum. The distributions are normalized to emergence frequency per day per square degree (1 square degree is approximately 150 Mm^2). Harvey and Zwaan (1993) also show distributions for rise and decline phases. All are consistent with a single power law with an offset that is dependent on the level of activity. Only the smallest regions, including ephemeral regions, deviate somewhat from this parameterization. The line near the bottom indicates the total observed range; bins with no regions are shown by symbols on this line.

a partition into “small” and “large” regions.

The area of bipolar regions is proportional to their flux content (Schrijver and Harvey, 1994), with an average flux density of 100 G to 150 G, depending on the instrument and calibration used, but apparently not on cycle phase or evolutionary phase of the region. The total amount of flux that emerges in regions of a size between A and $A + dA$ is therefore proportional to $A \cdot N_{\text{em}}(A)dA \propto A^{\alpha+1}dA$. With $\alpha + 1 \approx -1$, the distribution of emerging flux has no characteristic size scale: the large number of small regions and the fewer large ones all contribute significantly to the photospheric flux budget. Note that the power law description has to fail at both the small and large limit in order to prevent divergence of the flux integral.

The mean latitude of emergence for bipolar regions depends on the phase of the solar cycle. It does not depend on the size of the active regions, although the width of the latitude range within which flux emerges is larger for smaller regions, particularly on the poleward side of the mean emergence latitude. The band width for emergence peaks at cycle maximum. The mean latitude shifts from near 60° for the very early onset of a given cycle,

through 30° near cycle maximum, to the equator, which it reaches when the next cycle is well into the rise towards maximum. This pattern is the equivalent for emerging flux of the sunspot butterfly diagram. Note that subsequent “11-year” cycles overlap by as much as 5 or 6 years, so that the time interval during which only a single “cycle” is visible on the disk is limited to some 4 or 5 years (Harvey, 1993). The FWHM of the emergence band is about 20° – 25° in latitude, although at least half of the regions larger than 10 square degrees emerge within a 12° strip centered on the mean latitude, and more than half of the smaller regions within a 20° strip.

The flux contained in emerging regions disappears from them internally or by dispersal into the surrounding network. The relative importance of these two processes is not well known (e.g., Schrijver and Harvey, 1994), nor is the mechanism by which flux disappears from the photosphere (e.g., Zwaan, 1987). The decay takes over 70% of the total active-region lifetime (Harvey, 1993).

To interpret stellar atmospheric radiative losses one must know how many regions of a given size there are on the disk at any given time. That distribution, $N_{\text{pr}}(A)$, (Schrijver 1988) differs from $N_{\text{em}}(A)$ because the lifetime of the active regions increases with size. In fact, the decay rate, $|\dot{A}|/A$ – to first order independent of cycle phase – appears to decrease for increasing size, so that larger regions live disproportionately longer than small ones (Schrijver and Harvey, 1994). The distribution of sizes of regions present, $N_{\text{pr}}(A)$, is a monotonically decreasing function which has no typical length scale associated with it and simply scales up and down with cycle phase, as is the case for $N_{\text{em}}(A)$. The total flux content in regions of size A is given by $A \cdot N_{\text{pr}}(A)$, which is a distribution that peaks at approximately 2000 Mm^2 . Thus in terms of flux content in existing photospheric bipolar regions there does appear to be a typical size scale which may be useful when modelling, e.g., stellar rotational modulation. One should allow for the possibility, however, that this is in part a bias caused by the omission of increasingly more smaller and smaller regions from the Solar Geophysical Data listings from which $N_{\text{pr}}(A)$ was derived.

Stellar rotation causes the observed atmospheric radiative emission to change as the visible hemisphere slides across the stellar surface. The resulting signal is not periodic, however, because of the evolution of active regions. The life time of solar bipolar regions ranges from less than a day up to a few months, depending on the region, and increasing with its size. Only approximately 11% live as long as 1 rotation, and only 3% as long as 2 rotations (Harvey, 1993). Despite the relatively short life time of most of the active regions compared to the rotation period of the Sun, the rotational modulation does allow measurement of the period. This success can be attributed in part to the tendency of regions to emerge in space-time

clusters, or “nests,” in which successive regions occur with a high spatial coherence (Castenmiller et al. (1986) report that the nest dimension is often smaller than approximately 10° by 10°). The emergence frequency per unit available area for bipolar regions emerging within pre-existing regions is a factor of at least 22 higher than in the surroundings, and varies weakly in phase with the sunspot cycle (Harvey, 1993). All in all, 40% up to possibly 55% of all active regions emerge in nests. Nests last quite a long time: Castenmiller et al. (1986) find a most likely lifetime of 7 rotations, with some exceptional nests living as long as 15 rotations!

Interestingly, the size distribution of the set of regions emerging within existing regions is the same as that for regions emerging outside existing regions (Harvey and Zwaan, 1993). Due to the low-number statistics, it remains undetermined whether the distribution of sizes of “offspring” regions depends on the size of the “parent” regions (K.L. Harvey, priv. comm.).

5. Large-scale dispersal of magnetic flux

The disk-integrated emission originates only in part from the bipolar regions: dispersing flux that has escaped from them contributes to the ubiquitous network, which for the Sun constitutes the dominant component in all outer-atmospheric emissions but the coronal emission (see below, and Fig. 4). What do we know about the network component?

The magnetic flux in the photosphere is embedded in persistent large-scale flows and erratically changing convective flows, among them supergranulation. These flows interact with the flux, which in concert with the actions of deep-seated, large-scale velocity fields such as differential rotation and meridional flow results in its dispersal. Despite extensive study, the evolution of the supergranulation pattern and of the magnetic field embedded in it still defy a concise description. It is clear, however, that much of the magnetic field is collected into the regions of strong down flows or “sinks” (see, for instance, Spruit et al., 1990). Not all flux eventually collects in the strongest of these sinks, however, as is demonstrated by the existence of a partially outlined supergranular network on magnetograms and filtergrams in, for example, chromospheric spectral lines. The flux moves about continuously in the evolving supergranular network. Surprisingly, the resulting flux dispersal resembles ordinary diffusion on time scales sufficiently longer than the mean supergranular life time, provided that differential rotation and meridional flow are incorporated in the model (e.g., Sheeley, 1992, Wang and Sheeley, 1994).

Despite the apparent success of the description of flux dispersal as an ordinary diffusion process superposed on large-scale flows, there are inconsistencies between that model and observations. For one thing, estimates of

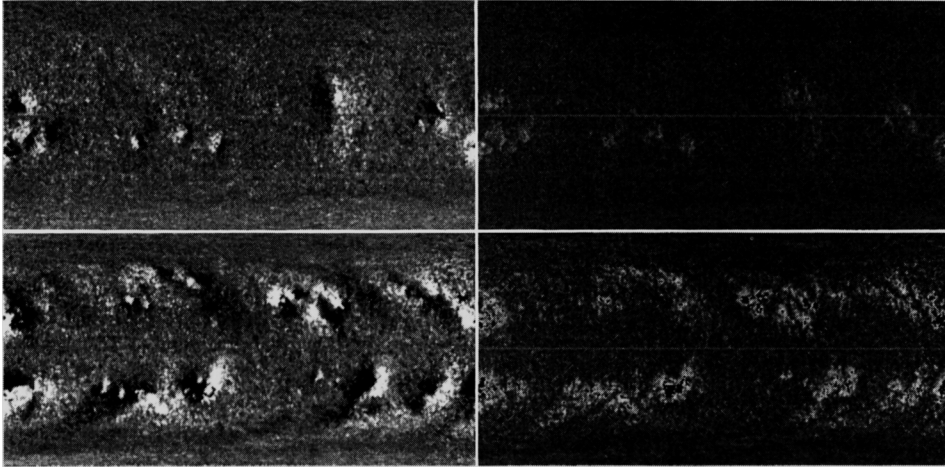


Figure 2. Examples of synoptic maps for the magnetic field (left) and for the Ca II H+K brightness (derived from the absolute value of the magnetic flux densities using a power-law relationship with exponent 0.6, e.g. Schrijver et al. 1989). The magnetic map is shown with enhanced contrast, between extremes of -15 and +15 gauss. The gray scale of the brightness map is proportional to the square root of the actual strength. The location of the equator is shown by a gray line. The top diagrams are for Carrington rotation 1764 (1985.25, near the end of Cycle 21), the bottom diagrams for rotation 1804 (1988.54, prior to the maximum of Cycle 22).

the diffusion coefficient range from 200–300 km²/sec for cross-correlation and tracking methods up to 600 km²/sec for large-scale simulations of flux dispersal (see Schrijver et al., 1996, for a list of references). Schrijver et al. (1996) suggest that this may be associated with a decrease of the rms velocity with increasing flux content of the concentrations of magnetic flux: as both cross-correlation and tracking methods predominantly track larger concentrations, these methods would systematically underestimate the mean dispersal rate for all flux.

The dispersal of flux is the result of diffusion, differential rotation, and meridional flow. The diffusion is large enough to allow some flux to cancel with opposite polarities at the equator. Much of the flux is, however, transported towards the poles, forming a pattern of poleward arches. Although this pattern is often shown as in the bottom lefthand panel of Fig. 2, one should realize a) that the gray scale is heavily weighted towards the low flux densities whereas most of the flux is actually within the much narrower latitude range of the activity belt proper, and b) that more irregular patterns such as shown in the top panel of that figure are more common. The simulations by Sheeley and colleagues properly describe these patterns (Sheeley, 1992, points out that the top 12% by size of the bipolar regions are active in the formation of these patterns), and explain their measured apparent

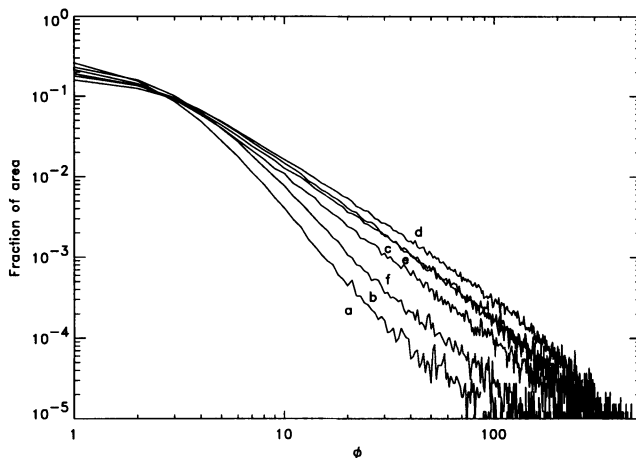


Figure 3. Time-dependent distribution function for the absolute magnetic flux density ϕ in synoptic maps with a resolution of 1 degree in longitude and 1/90 in sine latitude. The bin width is 1 gauss. The distribution functions are averages over five rotations, from cycle minimum (labelled 'a') to maximum ('d'). The rise and decline phases 'c' and 'e' have the same level of activity and comparable distribution functions.

rotation rates, including those of the nearly rigidly rotating coronal holes.

The successes of the passive diffusion-plus-flow model “seem to effectively rule out interpretations in terms of subsurface phenomena” (Sheeley, 1992): once the field has reached the photosphere and has escaped from whatever allows bipolar regions to survive as well-defined entities for some time, the field appears to move around passively, subject only to surface flows. This has severe implications on the connectivity and rigidity of the field: on the one hand the marked preference of bipolar regions to emerge with a slight tilt towards the equator (with a dispersion that increases for smaller regions, Harvey, 1993) and the size-independent mean emergence latitude suggest a strong connection to a deep-seated source region, but the passive response of network field to photospheric motions suggests a total severing of umbilical cords shortly after emergence. When interpreting stellar radiative losses, this severance may simplify the problem of understanding stellar radiative losses somewhat: one may be allowed to model flux dispersal in stellar photospheres by the same passive random walk, so that the source properties are the “only” unknowns.

6. The photospheric flux budget

Flux emergence, dispersal, and cancellation together determine the distribution of the magnetic field over the solar surface. Each of the magnetic el-

ements contributes to the total observed emission depending on its strength and its surroundings. The disk-integrated emission is therefore a weighted surface integral over the distribution function of magnetic flux. Examples of the distribution function are shown in Fig. 3. These distribution functions have some distinctive properties. First of all they show that most of the Sun is covered by weak network or by areas without any significant amount of intrinsically strong field. Secondly, the distribution functions change at all field strengths, thus a priori invalidating a simple, say, 2-component description that would incorporate only “active regions” and “network.” Thirdly, at the same global level of activity, there is no significant difference between distribution functions for phases of rising and falling activity: Schrijver and Harvey (1989) point out that noticeable hysteresis effects on the distribution function appear to be limited to less than the 5-month intervals over which they averaged the data. This not only says that the flux recycling happens rather quickly (related to this is the observation by Schrijver and Harvey (1994) that the total amount of flux that emerges in active regions is an order of magnitude larger than the amount of flux present at cycle maximum, which also requires that flux disappears from the photosphere on a time scale that is substantially shorter than the duration of the cycle), but also that the Sun at different phases of its cycle is a good proxy for stars of the same instantaneous activity level.

When combined with this third property, a fourth property of the distribution functions in Fig. 3, is of fundamental importance: the process of disk-averaging transforms the power-law relationships between radiative losses from the solar atmosphere observed with moderate spatial resolution into nearly identical relationships for disk-averaged values at different phases in the cycle. This property not only makes it possible to combine solar and stellar data to study stellar atmospheric structure, but also validates modelling stellar atmospheric emissions by a single-component atmosphere, as illustrated by the following.

Fig. 4 shows the simulated contributions of areas of different flux densities to the total emission from the Sun as a star. Near cycle maximum only about 40% of the total coronal emission comes from the quiet network with flux densities below 50 gauss, whereas 75% of the total chromospheric emission comes from these regions. This quantifies the problem that if one takes the emission from the Sun-as-a-star and models it by a simple spherically symmetric atmosphere, one tends to line up chromospheric emission that is weighted preferentially towards the network with coronal emission that is weighted preferentially towards plages. Despite this, the transformation from spatially-resolved to disk-averaged radiative losses is apparently such that disk-averaged emissions do correspond to some “average” magnetic feature somewhere on the disk.

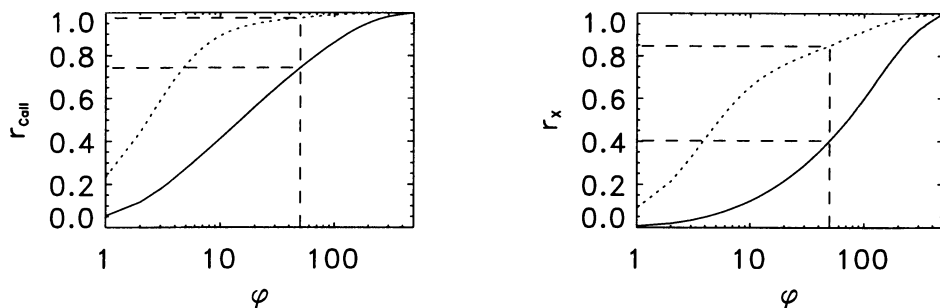


Figure 4. Simulated cumulative contributions in the chromospheric Ca II H+K (right) and coronal soft X-ray (left) emissions. The curves show the fractional contribution to the total emission from areas with absolute magnetic flux densities ϕ (at a spatial resolution of the order of a degree) below the corresponding threshold in ϕ . The emission strength was simulated using the distribution functions for the magnetic flux (shown in Fig. 3) for cycle minimum (dashed) and maximum (solid), and multiplying these with the expected emission (i.e. with $\phi^{0.6}$ for the chromospheric emission, see Schrijver et al. (1989), and $\phi^{1.2}$ for the coronal emission; the latter slope is raised somewhat over the roughly linear dependence argued for in Schrijver et al. (1989) because the relationship between soft X-ray and Ca II H+K fluxes appears to be somewhat steeper than assumed in that paper). Pixels with flux densities above 500 gauss, generally in sunspots, were ignored. The dashed lines identify the levels corresponding to a threshold of 50 gauss, which is a suitable contour level for plage regions (Schrijver et al., 1989), but which also includes some active network, particularly near cycle maximum.

7. Measuring the dynamo strength

At present we still do not know which properties of the atmospheric magnetic field are to be used to measure that elusive property one tries to describe by the term “dynamo strength.” Atmospheric activity of cool stars is most easily measured by the radiative losses from their outer atmospheres. The radiative losses from the outer atmospheres depend on the magnetic flux density in the underlying photosphere. From this it appears that one can estimate the average photospheric magnetic flux density in stars by measuring atmospheric radiative losses. This may not give us much grip on stellar dynamos, because the measurement of the amount of flux Φ present in the photosphere may only be the first step if, for instance, the rate of flux appearance, dispersal, and disappearance in stellar photospheres – i.e. the dynamics of the field – is also important to measure dynamo strength (e.g., Durney, 1995). Schrijver and Harvey (1994) point out that the cycle amplitude in the amount of flux present at any time in the photosphere is a factor of 3.5 while that in the flux emergence rate is a factor of about 8. The cause of this difference appears to be that flux disappears much faster from the photosphere at cycle maximum than at cycle minimum. If the rate of emergence and disappearance is important to measure dynamo strength, then we would require a model that can describe flux dispersal

and cancellation in order to be able to succeed for stars other than the Sun.

Schrijver and Harvey (1994) stress the importance of this problem by discussing the case of the most rapidly rotating stars. The outer atmospheric emission saturates in these stars. In interpreting this effect we cannot formally identify whether the saturation in atmospheric radiative losses is caused a) by a saturation in the heating mechanism (possibly because of the strong interaction of the field and the photospheric motions or because the maximum of large-scale kinetic energy is being extracted from the (sub-)photospheric turbulent convection), b) a shift in the balance between plage and spot fluxes (compare O'Dell et al., 1995), c) by an increased flux disappearance rate in the photosphere (because of an increased small-scale mixing or more erratic flux emergence pattern), or d) by an actual saturation in the deep-seated dynamo. Even if rather than radiative losses the surface magnetic flux densities for plage and network could be measured and would be seen to saturate for very rapidly rotating stars, we would still be in doubt as to what actually happens to the dynamo, because the last two possibilities would still remain valid options. The observational study of the dynamics of the solar photospheric field is crucial to address this problem, because it provides a model for flux dispersal and cancellation that could be extrapolated to higher activity, i.e. flux emergence rates.

8. Measuring surface differential rotation

The shift in the average emergence latitude may in principle allow measurement of the differential rotation. Donahue and Keil (1995) used a data base covering eight years of disk-integrated measurements of the solar Ca II K line in an attempt to demonstrate this potential by using solar data. Their plot of rotation period vs. time at first glance appears consistent with the equatorward drift of the main activity belt in each solar cycle, jumping towards higher rotation periods as a new cycle begins. Figure 5 compares their results in a different diagram with differential rotation rates measured using different tracers. Near the maximum of cycle 22, the mean rotation rate is indeed recovered. The data points contributing most to the impression that differential rotation was indeed successfully measured by Danahue and Keil, however, are the two points near the onset and maximum of cycle 22. The rotation rates they measured are significantly too low, however. The measurement for cycle minimum around 1987, when the new cycle 22 began to emerge at high latitudes, has a false alarm probability of 0.09 and could be deemed spurious. The other low-lying data point, however, has a false alarm probability of only 6×10^{-12} , the lowest in the set!

Earlier attempts to measure the surface differential rotation for the Sun as a star (see Donahue and Keil, 1995) had failed or proven inconclusive.

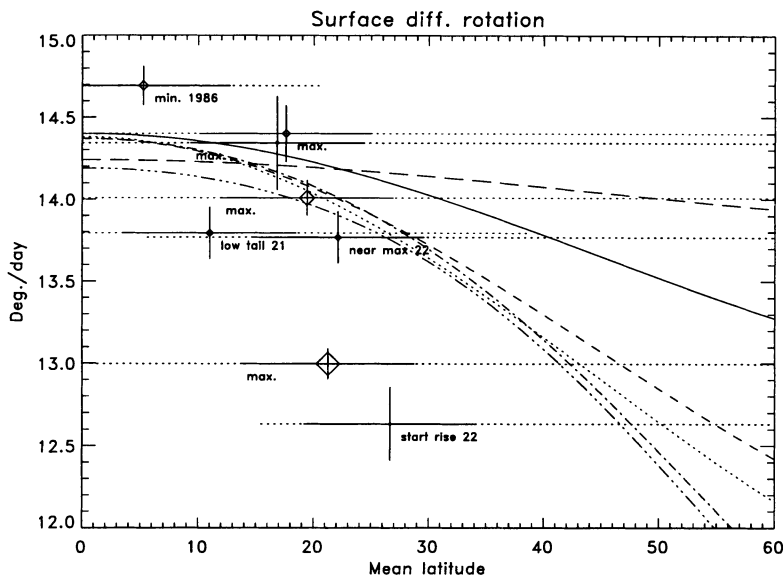


Figure 5. Solar surface differential rotation. Six curves show the solar rotation rate for magnetic features, coronal holes, spectroscopic data, etc. (from Snodgrass, 1992). The eight individual period measurements (assumed to be sidereal) and their uncertainties are taken from Donahue and Keil (1995; for one value a secondary peak in their periodogram analyses was used which is in better agreement with their trend) and plotted against the estimated mean latitude for flux emergence (taken in part from data for the preceding cycle from Harvey, 1993, assuming a similar behaviour for cycles 21 and 22). The symbol size increases with decreasing false alarm probability. The solid horizontal bars show the mean FWHM of the distribution of AR emergences. The dotted horizontal bars show the full width of the latitude range associated with the cycle (also from Harvey 1993).

Donahue and Keil (1995) used an observing window of 200 days, roughly equal to the Mt. Wilson Ca II H+K observing season of 120–180 nights, and substantially shorter than those used by the earlier authors. But even that appears to result in misleading data. The discrepancy between the observed and expected rotation rates for the Sun as a star is a warning that when a similar method is applied to measure stellar differential rotation for stars with rotation periods that are comparable to or longer than the evolutionary time scale of the set of large active regions that dominate the rotation signal, the results are to be interpreted with extreme caution. For stars with rotation periods of the order of a few days or at most one to two weeks, the effect of active-region evolution on surface differential rotation may be less severe, because the time-scale for active-region evolution is then likely to be shorter than the rotation period. On the other hand, the larger number of active regions will complicate the interpretation of the signal.

9. In conclusion

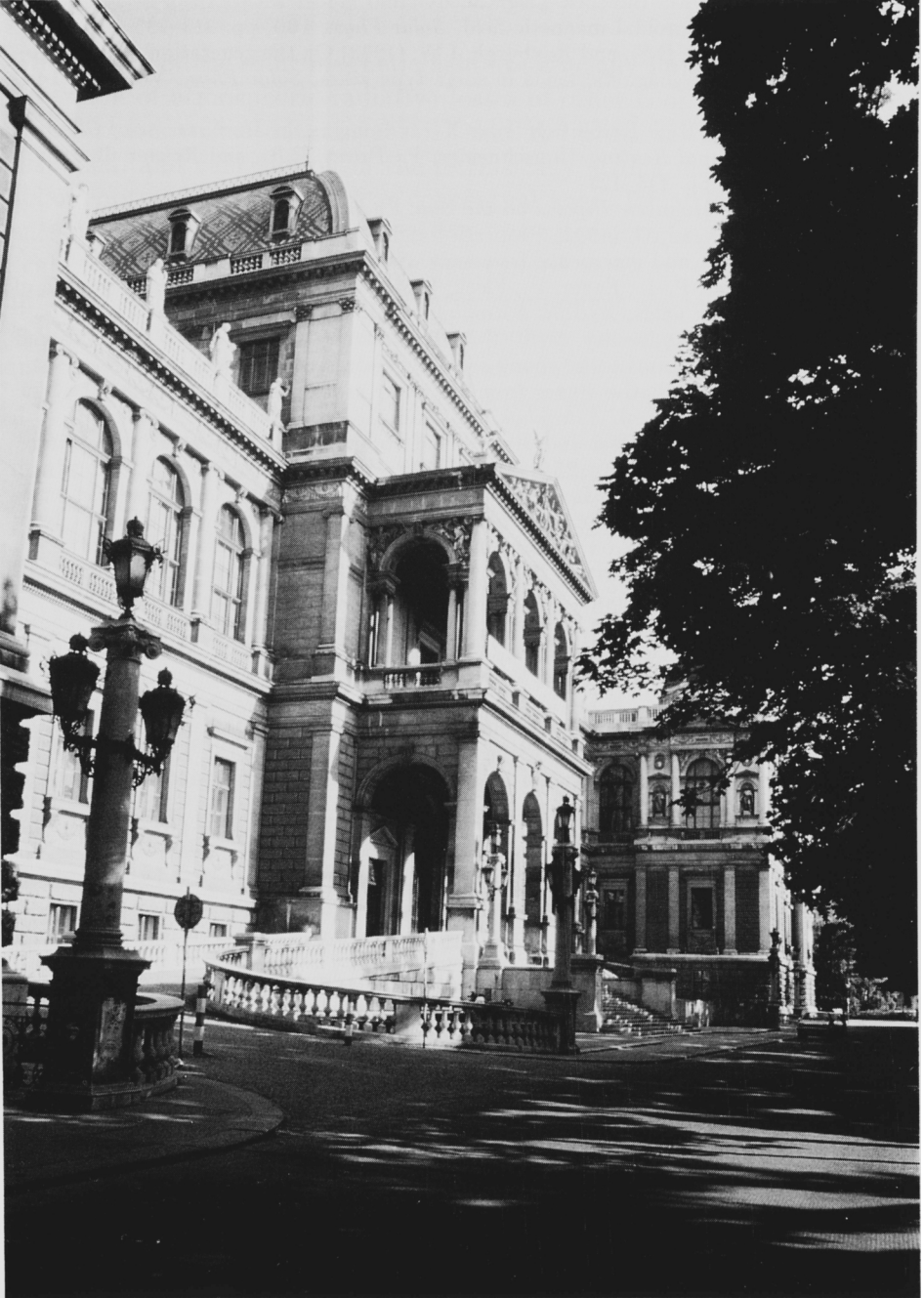
The details of the solar magnetic field are crucially important to the interpretation of atmospheric radiative losses of other cool stars. Comparisons of solar and stellar data suggest i) that the processes of flux emergence, dispersal, and cancellation of the intrinsically strong magnetic field in the solar photosphere are useful as conceptual bases for at least a substantial subset of cool stars, ii) that there does not appear to be a dominant length scale for active regions, iii) that one cannot think of stellar atmospheres in terms of a simplified two or three component model, iv) that the solar outer atmospheric processes and topology are a good starting point to interpret stellar radiative losses, v) that modelling stellar atmospheres using disk-integrated fluxes is to some extent valid, because these emissions appear to describe at least some existing feature on the star despite the nonlinearity of relationships between outer-atmospheric flux densities and the mixture of magnetic components on stellar surfaces, vi) that measuring the strength or amplitude of the internal dynamo may be difficult or intrinsically ambiguous, vii) that measuring surface differential rotation of stars with activity levels not too different from the Sun may not be feasible, and that it may be very difficult even for more active stars.

It appears that outer atmospheres of cool stars over a substantial range of stellar parameters are different blends of sets of features that may not differ all that much from their solar counterparts. If we can learn to understand the principles behind solar activity, we can therefore advance our understanding of stars. This does not mean we should cling to the solar example as the only useful and valid template, for clearly stars have surprises in store. But it does mean that we should always turn to the Sun to check our hypotheses and to verify what we can find there and what we cannot, thus making the Sun an integral part of stellar physics.

References

- Berger, T.E., and Title, A.M. (1995) On the dynamics of small-scale solar magnetic elements, *ApJ.*, in press
- Capelli, A., Cerruti-Sola, M., Pallavicini, R., Cheng, C.C. (1989) A comparison of solar and stellar ultraviolet spectra obtained with Skylab and IUE, *Astron. Astrophys.*, **Vol. no. 213**, pp. 226–244
- Castenmiller, M.J.M., Zwaan, C., van der Zalm, E.B.J. (1986) Sunspot nests. Manifestations of Sequences in Magnetic Activity, *Solar Phys.*, **Vol. no. 105**, pp. 237–256
- Donahue, R.A. (1993) *Surface Differential Rotation in a Sample of Cool Stars*. Ph.D. Thesis, New Mexico State University, Las Cruces, New Mexico.
- Donahue, R.A. and Keil, S.L. (1995) The solar surface differential rotation from disk-integrated chromospheric fluxes, *Solar Phys.*, **Vol. no. 159**, pp. 52–62
- van Driel-Gesztelyi, L., van der Zalm, E.B.J., and Zwaan, C. (1992) Active nests on the Sun, in *The Solar Cycle*, K.L. Harvey (ed.). Astron. Soc. of the Pacific Conf. Series, **Vol. 27**, pp. 89–96, ASP, San Francisco.

- Durney, B.R. (1995) On a Babcock–Leighton dynamo model with a deep-seated generating layer for the toroidal magnetic field, *Solar Phys.*, **160**, pp. 213–235
- Durney, B.R., de Young, D.S., and Roxburgh, I.W. (1993) On the generation of the large-scale and turbulent magnetic fields in solar-type stars, *Solar Phys.*, **Vol. no. 144**, pp. 207–225
- Golub, L. (1991) Very High Resolution Solar X-ray Imaging, in *Mechanisms of Chromospheric and Coronal Heating*, Ulmschneider, P., Priest, E.R., and Rosner, R. (eds.), Springer-Verlag. pp. 115–123
- Harvey, K.L. (1993) *Magnetic Bipoles on the Sun*. Ph.D. Thesis, Univ. of Utrecht
- Harvey, K.L., and Zwaan, C. (1993) Properties and emergence of bipolar active regions I. Size distribution and emergence frequency, *Solar Phys.*, **Vol. no.148**, pp. 85
- Keller, C.U., Deubner, F.-L., Egger, U., Fleck, B., Povel, H.P. (1994) On the strength of solar intra-network fields, *Astron. Astrophys.*, **Vol. no. 286**, pp. 626–634
- O’Dell, M.A., Panagi, P., Hendry, M.A., Collier Cameron, A. (1995) New observational limits on dynamo saturation in young solar-type stars, *A&A*, **294**, pp. 715
- Schrijver, C.J. (1988) Radiative fluxes from the outer atmosphere of a star like the Sun: a construction kit, *Astron. Astrophys.*, **Vol. no. 189**, pp. 163–172
- Schrijver, C.J. (1992) The basal and strong-field components of the solar atmosphere, *Astron. Astrophys.*, **Vol. no. 258**, pp. 507–520
- Schrijver, C.J. (1993) Relations between the photospheric magnetic field and the emission from the outer atmosphere of cool stars III. The chromospheric emission from individual flux tubes, *Astron. Astrophys.*, **Vol. no. 269**, pp. 395–402
- Schrijver, C.J. (1995) Basal heating in the atmospheres of cool stars; observational evidence and theoretical support, *Astron. Astrophys. Rev.*, **Vol. no. 6**, pp. 181–223
- Schrijver, C.J., Coté, J., Zwaan, C., Saar, S.H. (1989) Relations between the photospheric magnetic field and the emission from the outer atmosphere of cool stars. I. The solar Ca II K line core emission, *ApJ.*, **Vol. no. 337**, pp. 964–976
- Schrijver, C.J., and Harvey, K.L. (1989) The distribution of solar magnetic fluxes and the nonlinearity of stellar flux–flux relations, *ApJ.*, **Vol. no. 343**, pp. 481–488
- Schrijver, C.J., Zwaan, C., Balke, A.C., Tarbell, T.D., Lawrence, J.K. (1992) Patterns in the photospheric magnetic field and percolation theory, *Astron. Astrophys.*, **Vol. no. 253**, pp. L1–L4
- Schrijver, C.J., and Harvey, K.L. (1994) The photospheric magnetic flux budget, *Sol. Phys.*, **Vol. no. 150**, pp. 1–18
- Schrijver, C.J., Shine, R.A., Hagenaar, H.J., et al. (1996) Dynamics of the chromospheric network I. Mobility, dispersal, and diffusion coefficients, submitted to *ApJ*.
- Sheeley, N.R. (1992) The flux transport model and its implications, in *The solar cycle*. A.S.P. Conf. Series, Vol. 27, Astron. Soc. of the Pac., San Francisco. pp. 1–13
- Snodgrass H.B. (1992) Synoptic observations of large scale velocity patterns on the Sun, in *The solar cycle*, K.L. Harvey (ed.), Astron. Soc. of the Pac. Conf. Series **Vol. no. 27**, pp. 205–240
- Solanki, S.K., Steiner, O., and Uitenbroek, H. (1991) Two-dimensional models of the solar chromosphere, *Astron. Astrophys.*, **Vol. no. 250**, pp. 220
- Spruit, H.C., Nordlund, Å, Title, A.M. (1990) Solar Convection, *ARAA*, **Vol. no. 28**, pp. 263–301
- Steiner, O., Knölker, M., and Schüssler, M. (1994) Dynamic interaction of convection with magnetic flux sheets: first results of a new MHD code, in *Solar Surface Magnetism*. R.J. Rutten and C.J. Schrijver (eds.), Kluwer Academic Publishers. pp. 441–470
- Ulmschneider, P., Priest, E.R., and Rosner, R. (1991) editors of *Mechanisms of Chromospheric and Coronal Heating*. Springer-Verlag.
- Wang, Y.-M., and Sheeley, N.R. (1994) The rotation of photospheric magnetic fields: a random walk transport model, *ApJ*, **Vol. no. 430**, pp. 399–412
- Zwaan, C. (1987) Elements and patterns in the solar magnetic field, *ARAA*, **Vol. no. 25**, pp. 83–111



The meeting location: The University of Vienna, founded 630 years ago in 1365 by Rudolf IV., houses today approximately 70,000 students and the Institute for Astronomy in the 18th Viennese district (see also page 288).